RESEARCH ARTICLE

Developmental Dynamics
DOI10.1002/dvdy.82

# Title: Developmental control of convergent floral pigmentation across evolutionary timescales

Maximilian Larter[1], Amy Dunbar-Wallis[1], Andrea E. Berardi[12], and Stacey D. Smith[1].

[1]Department of Ecology and Evolutionary Biology, University of Colorado-Boulder, CO, USA
[2]Institute of Plant Sciences, University of Bern, Switzerland

**Corresponding author**: Maximilian Larter: Email: maximilian.larter@colorado.edu.
C177, Ramaley Hall. 1800 Colorado Ave. Boulder, CO 80309-0334 USA.
Telephone: 720-401-3287.

**Running title:** Multiple mechanisms drive convergence

**Bullet points:**

- Different genetic and developmental mechanisms can underlie convergent phenotypic evolution at different timescales
- We describe convergent losses of floral anthocyanin pigments within and among species
- Gene expression changes are responsible for losses at the species level, with a distinct developmental mechanism in the white morphs within species

**Keywords**: anthocyanin; convergence; flavonol; qPCR; PGLS; principal component analysis

**Grant sponsor:** National Science Foundation. Grant number DEB1355518.


Received: Mar 18, 2019;Revised: Jun 18, 2019;Accepted: Jun 21, 2019

**Abstract:**

Background: Convergent phenotypic evolution has been widely documented across timescales, from populations, to species, to major lineages. The extent to which convergent phenotypes arise from convergent genetic and developmental mechanisms remains an open question, although studies to-date reveal examples of both similar and different underlying mechanisms. This variation likely relates to a range of factors, including the genetic architecture of the trait and selective filtering of mutations over time. Here we focus on floral pigmentation, and examine the degree of developmental convergence between white-flowered lineages and white morphs within pigmented species.

Results: Using the model clade Iochrominae, we find that white morphs and white-flowered species are biochemically convergent, sharing an absence of colorful anthocyanin pigments. Regression analyses suggest that the expression levels of upstream genes are the strongest drivers of total pigmentation across species, although white species also show sharp downregulation of the downstream genes. The white morphs do not share this pattern and present overall expression profiles more similar to the pigmented species.

Conclusions: These results suggest that the mechanisms underlying variation within populations differ from those which give rise to fixed differences between species. Future work will aim to uncover the genetic changes responsible for this developmental non-convergence.

## Introduction

Understanding how genetic and developmental differences shape phenotypic variation within and between species is a key question in evolutionary biology. Significant progress has been made in identifying loci associated with trait variation, and these studies (surveyed in Martin and Orgogozo 2013) have revealed dramatic examples of genomic 'hotspots' that have been involved repeatedly in the evolution of similar phenotypes in different taxa. Moreover, the types of changes appear to show some predictable patterns, with *cis*-regulatory mutations more commonly contributing to morphological variation between species than coding sequence mutations (Stern and Orgogozo, 2009). This pattern is consistent with the notion that *cis*-regulatory mutations often result in fewer negative pleiotropic consequences and thus are more likely to become fixed over longer evolutionary timescales, giving rise to differences between species and higher taxa (Wray, 2007; Carroll, 2008). Nonetheless, relatively few studies have compared the mechanisms underlying trait variation within and between closely related species (e.g., Whittall et al. 2006; Wittkopp et al. 2009; Rogers et al. 2013; Massey and Wittkopp 2016), limiting our ability to assess the strength of this selective filtering of mutations (Gompel and Prud'homme, 2009).

Given the frequency of color variation in nature and its close connection to biochemical pathways, pigmentation provides a valuable trait for studying the mechanisms of phenotypic evolution across timescales (Kopp, 2009; Sobel and Streisfeld, 2013). In animal systems, melanin synthesis has been studied in depth, and this detailed knowledge of biochemistry and genetics has allowed for comparative studies, revealing similar mechanisms of evolutionary change across taxa (Wittkopp and Beldade, 2009; Hubbard et al., 2010). In plant systems, flavonoid pigments (including the colorful anthocyanidin-based compounds) have played an analogous role in connecting genotype to phenotype. As with melanin biosynthesis, the biochemical steps and transcriptional regulators of the flavonoid pathway are widely conserved

(Rausher, 2006; Albert et al., 2014), making it feasible to identify the genetic and developmental basis for new phenotypes in non-model organisms (Sobel and Streisfeld, 2013).

Here we leverage previous work on floral flavonoid production to examine the developmental basis for convergent losses of floral anthocyanin pigmentation within and between species. Anthocyanins are responsible for red, blue, and purple colors in most flowering plants (Winkel-Shirley, 2001; Grotewold, 2006), and mutations that disrupt their production result in white to yellow flowers, depending on the background levels of yellow carotenoids and flavonoid co-pigments (Whittall et al., 2006; Tanaka et al., 2008; Cooley et al., 2011). Fixed losses of floral anthocyanin pigmentation are perhaps among the best studied phenotypic transitions in plants, and they appear to consistently involve mutations in the MYB transcription factors that regulate the downstream steps of the pathway, e.g., DFR and ANS (Fig. 1) (Sobel and Streisfeld, 2013; Gates et al., 2017). While there are fewer analyses of segregating 'acyanic' (white or yellow) morphs within pigmented species, studies-to-date point to a wider range of causal changes including both *trans*-regulatory mutations and loss-of-function mutations in enzyme-coding genes (Chang et al., 2005; Wu et al., 2013; Coburn et al., 2015).

Building on existing knowledge of the flavonoid pathway (Fig. 1) and its role in flower color, we examine pathway gene expression and floral pigmentation in the Andean clade, Iochrominae (Solanaceae). In this mostly purple-flowered clade, some species have completely lost floral anthocyanin pigmentation, resulting in white or yellow flowers (Fig. 2). Additionally, several of the normally pigmented species present occasional white or yellow morphs within populations, allowing us to compare the genetic mechanisms behind losses both above and below the species level. For simplicity, we will refer to the pale (white or yellow) phenotypes as 'white' throughout the paper. We quantified the production of the two major classes of flavonoids in Iochrominae (anthocyanins and flavonols; Berardi et al. 2016) along with the expression of core structural genes in the pathway in order to address the following questions: (i) are the white morphs convergent with the white species at the biochemical level (i.e., do they have similar anthocyanin

and flavonol profiles)? (ii) how does the expression of pathway genes relate to flavonoid production within and among species? and (iii) do the white morphs show patterns of gene expression similar to white species, consistent with a similar genetic basis? Our results suggest that, while shifts from purple to white flowers at the species level are driven by changes in gene expression, segregating variation within species involves distinct developmental mechanisms. These findings point to the need for additional research to understand how segregating variation within populations translates to fixed differences between species.

## Results

### *Biochemical convergence above and below the species level*

In keeping with the diversity of flower hue and intensity found in Iochrominae (Smith and Baum, 2006), floral anthocyanin and flavonol concentration varied widely across the Iochrominae clade (Fig. 2). Among the pigmented species, we found approximately 10-fold variation in anthocyanin concentration (0.06 to 4.1 mg/g), with the lilac flowers of *Eriolarynx lorentzii* at the low end of the range and the nearly black flowers of *Iochroma parvifolium* having the highest values (Fig. 2). In flowers of the seven white species, such as *I. ellipticum* and *I. arborescens*, we could not detect any anthocyanidin production (Fig. 2). Most pigmented and white species produced flavonol co-pigments (with the exception of *I. ellipticum*). The range of flavonol production was also broad (0.003 to 3.7 mg/g), with similar ranges between the pigmented (0.05-3.7mg/g) and white (0.003-1.05 mg/g) species. We did not find a significant negative correlation between anthocyanidins and flavonols (Fig. 3) although this pattern has been observed in experimental systems (Gerats et al., 1982; Davies et al., 1997; Yuan et al., 2016).

The flavonoid profiles of the white morphs of the pigmented species were similar to those of the white species, suggesting the phenotypic convergence is coupled with biochemical convergence.

For two of the six polymorphic species (Table 1), the white morphs produced no detectable anthocyanidins (Fig. 2). In the remaining cases, only trace amounts were produced (< 0.08 mg/g), corresponding to on average 40-fold less than the pigmented conspecifics. The range in flavonol content across the morphs was similar to that observed across the white and pigmented species (Fig. 2; 0.2 to 4.1 mg/g). Thus, both white species and white morphs of normally pigmented species vary in flavonol production, but share the convergent loss of anthocyanins.

*Relationship between pathway gene expression and phenotypic variation*

We next used phylogenetic regression analyses to estimate the relationship between the observed variation in floral flavonoids and the expression of core enzymes of the pathway. At the species level, pigmented species fall within a restricted range, with roughly 100-fold variation in expression level for all of the genes (data for two example genes shown in Fig. 4). By contrast, the white species vary dramatically, with up to 10,000-fold difference in the expression of downstream genes compared to the pigmented species (see also Larter et al. 2018). Across both pairwise and multiple regressions (Table 2), we estimated that the best model for anthocyanidin and flavonol concentration (more than 10 AIC units lower than competing models) included only the expression of *Chi* (Fig. 4), an upstream gene in the pathway (Fig. 1). The result is consistent with theoretical work showing that upstream enzymes exert greater control over total flux through the pathway (Wright and Rausher, 2010; Rausher, 2013). Despite the sharp downregulation of downstream genes in white species (Larter et al., 2018), these genes do not rank as strong predictors (Table 2), likely because most of the anthocyanidin and flavonol variation to be explained in the dataset falls within the pigmented species (Figs. 2, 3).

Compared with the marked separation between white and pigmented species for downstream genes, we found white morphs generally mixed with their pigmented conspecifics in terms of gene expression. For example, expression levels for the downstream gene *Ans* for the white morphs fell largely within the range of the pigmented species and were higher than those for

white species (Fig. 4). The similarity in gene expression between white and purple morphs is also apparent in within-species comparisons (Fig. 5). We did observe several exceptions to this pattern: *F3h*, *Dfr* and *Ans* in *I. cyaneum*, *Chi* and *Dfr* in *I. calycinum*, and *Chi* and *Ans* in *I. parvifolium*, which all had lower expression in the white morphs (Fig. 5). It is worth noting however that for the latter two species, we were only able to locate a single white morph and thus we lack biological replication to estimate uncertainty in those expression values. We also found that *Chs* expression in *Saracha punctata* was significantly higher in the white morphs than in the pigmented individuals, which could explain the higher concentration of flavonols in the white morphs (Fig. 2).

*Developmental non-convergence of white species and white morphs*

In order to summarize the differences in gene regulation across color morphs and species for the entire pathway, we carried out phylogenetic principal components analysis (pPCA) on the expression data for five core pathway genes (*Chs*, *Chi*, *F3h*, *Dfr*, and *Ans*, Fig. 1). The first two principal components together capture 83% of the variation in gene expression. Consistent with the patterns from analyses of individual genes (Figs. 4, 5), we found that the white morphs cluster with the pigmented species and are separated from the white species in pPC space (Fig. 6A). The loadings of each gene onto the pPC axes revealed that this division between the white species and the pigmented species plus white morphs is largely driven by the expression of the downstream genes (*Dfr*, *Ans*), whose expression is tightly correlated (Larter et al. 2018). The remaining upstream genes also appear correlated (Fig. 6B), but their axis of variation does not align with the separation of white species from the rest.

**Discussion**

With a large and increasing set of phenotypes for which the genetic basis is well-understood (Martin and Orgogozo, 2013), the field of evo-devo has begun to move from addressing fundamental mechanistic questions towards testing hypotheses based upon those mechanisms

(Stern, 2011; Nunes et al., 2013). For example, with the observation that the MC1R locus has been repeatedly involved in pigmentation differences within and among species, we can turn to testing the factors that might drive this evolutionary pattern, e.g., mutation rates and target size (Hubbard et al., 2010). Among the factors which might predict the loci of evolution, pleiotropy has received perhaps the greatest attention (e.g., Stern 2000; Streisfeld and Rausher 2011), although the strength of this relationship may vary across traits and timescales (Stern and Orgogozo, 2009). Gompel and Prud'homme (2009) present a specific evolutionary prediction with respect to timescales, namely that selection will have a 'funneling' effect, pruning away mutations with negative pleiotropic consequences and leaving only a subset which can move to fixation. This funneling process would be expected to manifest in comparisons of the genetic basis for phenotypic variation within populations and between species, although few systems have a sufficiently deep literature for a formal assessment (Streisfeld and Rausher, 2011; Massey and Wittkopp, 2016).

In plant systems, flavonoid-based pigmentation is a model trait for evo-devo studies (Kopp, 2009; Sobel and Streisfeld, 2013), and our results in Iochrominae suggest that it will provide a powerful system for testing the hypothesis of pleiotropy-driven selective filtering of mutations. Similar to many flowering plant clades, Iochrominae displays wide inter- and intraspecific variation in flower color, much of it driven by differences in flavonoid type and amount (Coburn et al., 2015; Berardi et al., 2016; Larter et al., 2018). Our flavonoid profiling confirms that the white morphs that appear periodically in populations of normally pigmented species share the same biochemical signature as white species, i.e., they lack the colorful anthocyanins while still producing the upstream flavonols (Figs. 1, 2, 3). This biochemical change is tightly associated with downregulation of downstream genes (DFR, ANS) in the white species (Gates et al., 2017; Larter et al., 2018) but not in the white morphs (Figs. 4, 5). Instead, the overall expression patterns for white morphs are most similar to their pigmented counterparts (Figs. 5, 6). Indeed, the morphs are largely nested within the 'expression space' of the pigmented species, which is separate from that of the white species (Fig. 6).

The developmental difference between these visibly and biochemically convergent phenotypes above and below the species level points to a distinct genetic basis, although further work would be required to identify the precise mutations in each case. Nevertheless, previous studies in Iochrominae and other clades are consistent with differing causal mutations underlying segregating and fixed losses of floral anthocyanins. For example, a loss-of-function mutation in the coding region of DFR appears to be responsible for the bright white morph of *Iochroma calycinum* (Fig. 2, Coburn et al. 2015; see Wu et al. (2013) for a similar case in *Mimulus*). Acyanic morphs have also been linked with *cis*-regulatory and coding sequence mutations in other enzyme-coding genes (Coberly and Rausher, 2003; Dick et al., 2011) and transcription factors (Chang et al., 2005) in several plant groups. By contrast, fixed species-level losses of floral anthocyanins across multiple clades have uniformly been attributed to mutations in MYB transcription factors, which coordinately downregulate multiple pathway genes (Sobel and Streisfeld, 2013). For instance, the shift from purple to white flowers in the *I. loxense* lineage (pictured in Fig. 2) was caused by a dominant gain-of-function mutation in an R3 MYB repressor, resulting in losses of DFR and ANS expression (Gates et al., 2017). This bias toward fixation of mutations in MYB transcription factors has been attributed to their high specificity (in terms of DNA targets, tissues and timing), which presumably results in lower potential for deleterious pleiotropy (Sobel and Streisfeld, 2013).

Patterns in the biochemical profiles and expression data can provide additional hints regarding the range of mutations that may have given rise to the white morphs in some Iochrominae species. We can consider two broad classes of mutations: coding sequence mutations in the enzymes of the pathway and regulatory mutations (either in *cis*-regulatory elements or in transcription factors controlling the pathway). With respect to coding mutations, we note that all of the white morphs produce flavonols, which require the activity of CHS, CHI and F3H (Fig. 1). Thus, loss of function mutations in these upstream genes are unlikely to be involved the evolution of white flower phenotypes. Indeed, mutations at CHS, CHI and F3H are thought to be highly pleiotropic as they affect the entire flavonoid pathway (Rausher et al., 1999) and only one

naturally occurring loss of function mutation is known among these three loci (CHS in *Ipomoea purpurea*; Coberly and Rausher 2003). By contrast, the downstream genes experience higher rates of substitution (Rausher et al., 1999), and loss-of-function mutations in DFR are known to segregate within populations (Wu et al. 2013; Coburn et al. 2015). By eliminating enzyme activity, such mutations completely block anthocyanin production, as seen in the rare white morphs of *I. calycinum* and *I. parvifolium* (Fig. 2).

While losses of pathway gene expression underlie white morphs in other taxa (e.g., Coberly and Rausher, 2003; Cooley et al., 2011; Dick et al., 2011), it is unclear if the levels of downregulation we document for most white morphs would be sufficient to produce a white phenotype. For example, the white morphs of *E. fasciculata* and *S. punctata* show a trend toward decreased expression of the downstream genes (roughly 3 to 5-fold downregulation on average) relative to their pigmented conspecifics (Fig. 5), but these values pale in comparison to the degree of downregulation observed in white species (ca. 1000-fold, Fig. 4). The white morphs of *I. cyaneum* represent an exception to this general pattern of minor expression differences between white and pigmented conspecifics. In this species, the white morphs are nearly 100-fold down-regulated for *Dfr* and *Ans* relative to the purple-flowered individuals (Fig. 5) and sit nearest the white species in expression space (Fig. 6). The coordinated downregulation of these two genes is consistent with a mutation in their shared MYB transcriptional regulators (Gates et al., 2017). Although the expression differences in the remaining taxa appear too minor to drive a loss of pigmentation alone, it is important to note that white morphs might arise through the combined action of multiple segregating regulatory or coding mutations. For example, a coding mutation that reduces DFR efficiency together with a *cis*-regulatory mutation that lowers floral *Ans* expression might together result in a white flower when neither alone results in the phenotype. The frequency of such mutations will, in turn, influence the occurrence of the white morphs, which in Iochrominae range from exceptionally rare (<1%) to extremely common (<50%) (Table 1).

Returning to Gompel and Prud'homme's (2009) selective funnel, we can now consider how segregating variation within species translates to fixed species differences in flower color. Ultimately, all species differences must begin as a mutation in a single individual, and thus must have at some point been present as polymorphisms within species. Yet, at least in Iochrominae, the present polymorphisms have a distinct developmental, and presumably genetic, basis from the species differences. One possible explanation for this disconnect is that the class of mutations that are able to persist and become fixed (e.g., gain- or loss-of-function mutations in the MYB genes) are rare relative to the suite of regulatory and coding mutations that produce a viable pale-flowered individual. This aligns with surveys of spontaneous mutations (5/78 or 6% in MYB genes; Streisfeld and Rausher, 2011), although it is unclear if this pattern holds in nature. Alternately, the developmental convergence seen in the four independent white lineages might be the result of an accumulation of fixed mutations (even if they all correspond to a single locus; Gates et al., 2017) that progressively reduced the downstream gene expression and stabilized the novel phenotype. Ultimately, a broader sampling of white morphs along with a more detailed dissection of molecular mechanisms for convergence across levels will be required to distinguish among these and other possibilities. Nevertheless, our results reveal that, while the developmental bases for losses of floral pigmentation are highly convergent across species, this predictability breaks down within species, highlighting the need for continued research in evo-devo at the boundary of micro- and macroevolution.

## Experimental Procedures

### *Plant material*

Flower buds for gene expression analyses were collected from the field for 19 species and the white morphs from the natural range of Iochrominae in western South America. During these field trips, we surveyed flower color variation in local herbaria and natural populations to locate white morphs and to obtain a rough estimate of their frequency compared to pigmented morphs.

Samples for an additional nine species were collected from greenhouse plants grown from seed in Boulder, Colorado (USA), giving us a total of 28 species. These plants were placed outside of the greenhouse prior to bud collection to simulate natural light conditions and maximize pathway activity. All buds were collected at a stage roughly equivalent to *Petunia* bud Stage 5 (Pollak et al., 1993), at which point floral pigmentation is developing and both the early and late genes of the pathway are expressed (Smith and Rausher, 2011).We also collected flower tissue from the same set of individuals for HPLC; this tissue was dried in silica gel and stored at -80°C until extraction. Each species is represented by three individuals, except *Vassobia breviflora* (two individuals) and *Iochroma ellipticum* (one individual). In addition, we sampled up to three acyanic morphs for each of the polymorphic species (Table 1). For the HPLC measurements, we were only able to include one individual of *I. cornifolium* and two individuals for *I. amicorum* and *Saracha punctata*. Voucher information for all individuals included in this study is available in the associated Dryad Digital Repository: https://doi:10.5061/dryad.p5dq84v.

*Flavonoid identification and quantification*

We used High-Performance Liquid Chromatography (HPLC) to identify and quantify concentrations of major classes of flavonoids found in Iochrominae flowers: anthocyanidins, flavonols, and flavones (Berardi et al. 2016). Following Berardi et al. (2016) and Larter et al. (2018), we extracted flavonoids from dried floral tissue with the acid hydrolysis method, which converts the many glycosylated anthocyanins into the core anthocyanidins (Harborne, 1998). The extracts were then re-suspended in methanol and analyzed with an Agilent Infinity 1260 HPLC system. Peaks at 520 nm for anthocyanidins and at 360 nm for flavonols and flavones were used to identify compounds using retention times and absorbance spectra, comparing them to commercial standards (Extrasynthese, Genay, France). Chromatograms were analyzed in the Agilent Chemstation software to obtain peak area for each compound in each sample. These areas were then compared to dilution series of the standards to obtain concentrations (mg compound per g dried floral tissue weight). We used a log(x+1) transformation prior to analyses.

*Quantitation of gene expression*

Gene expression data for individuals of the pigmented and white species was taken from our previous work (Larter et al., 2018). We obtained new data for white morphs within pigmented species for this study (Table 1) using the same procedure and analysis methods (Larter et al., 2018). Briefly, floral buds were collected and preserved using RNAlater (Quiagen, Valencia, CA). Total RNA was extracted using the Spectrum kit (Sigma–Aldrich, St. Louis, MO) with on-column DNase digestion (Qiagen). We synthesized cDNA using SuperScriptII Reverse Transcriptase (Life Technologies, CA), and amplified gene fragments using previously designed primers for flavonoid genes and a reference "housekeeping" gene, the elongation factor EF1-α (Coburn et al., 2015). Three replicate amplification curves per individual were analyzed in R (R Core Team, 2019), and from the log-linear phase of the curve, we obtained parameters for the relative expression ratio model (Pfaffl, 2001; Peirson et al., 2003). As in Larter et al. (2018), expression of each gene was first normalized by the expression of EF1-α. We then calculated $\log_{10}$ fold-change relative to expression in a single purple-flowered reference individual of *Iochroma cyaneum*, which was included in every qPCR experiment as a control. Thus, each unit on the log fold-change scale represents a 10-fold increase or decrease in transcript concentration relative to the reference individual, and 0 represents equal expression to the reference. The choice of a reference individual is arbitrary, but provides some intuitive interpretation (i.e., we expect that unpigmented species or morphs might show negative fold changes for one or more pathway genes relative to this purple-flowered reference).

*Statistical comparative methods*

We estimated the relationship between gene expression and anthocyanin and flavonol production using phylogenetic comparative methods, which account for the non-independence due to shared evolutionary history (Dunn et al., 2013). These analyses included the entire dataset of 28 species. To incorporate within species variation into the phylogenetic regression models, we used

the PGLS Ives method (Ives et al., 2007; Lavin et al., 2008). This method incorporates a phylogenetic covariance matrix into the model and uses branch-length transformation to model trait evolution under the Ornstein-Ulhenbeck model. We used the branch lengths and topology from the maximum clade credibility tree of Iochrominae from Smith and Goldberg (2015) for these analyses. Parameter values were estimated using Restricted Maximum Likelihood, and their confidence intervals were calculated from 1000 parametric bootstraps. We also used functions from the {phytools} package (Revell, 2012) in R to visualize trait variation across the phylogeny (Fig. 2).

We carried out phylogenetic principal components analysis (pPCA) (Revell, 2009) as implemented in the {phytools} package. For the individual level phylogenetic PCA, we constructed a tree with new tips for each individual, created as polytomies with individual branch lengths equal to 1% of the initial species branch, following Berardi et al. (2016). This results in very shallow polytomies while preserving 99% of the length of the species-level branch. R code and data used in this study are available from the Dryad Digital Repository: https://doi:10.5061/dryad.p5dq84v.

**Acknowledgements**

This work was supported by National Science Foundation grant DEB1355518 to SD Smith. We are thankful to the authorities in Peru and Ecuador for granting permits (Nº 0259-2016-SERFOR-DGGSPFFS and Nº 05-2012- IC- FAU-DPAP-MA, respectively) to carry out sampling for this work. We also thank Theodore Garland and Anthony Ives for providing us with the MATLAB code for the phylogenetic regressions and for helping with the program usage.

**References**

Albert NW, Davies KM, Lewis DH, Zhang HB, Montefiori M, Brendolise C, Boase MR, Ngo H, Jameson PE, Schwinn KE. 2014. A Conserved Network of Transcriptional Activators and Repressors Regulates Anthocyanin Pigmentation in Eudicots. Plant Cell 26:962–980.

Berardi AE, Hildreth SB, Helm RF, Winkel BSJ, Smith SD. 2016. Evolutionary correlations in flavonoid production across flowers and leaves in the Iochrominae (Solanaceae). Phytochemistry 130:119–127.

Carroll SB. 2008. Evo-Devo and an Expanding Evolutionary Synthesis: A Genetic Theory of Morphological Evolution. Cell 134:25–36.

Chang SM, Lu Y, Rausher MD. 2005. Neutral evolution of the nonbinding region of the anthocyanin regulatory gene Ipmyb1 in Ipomoea. Genetics 170:1967–1978.

Coberly LC, Rausher MD. 2003. Analysis of a chalcone synthase mutant in *Ipomoea purpurea* reveals a novel function for flavonoids: Amelioration of heat stress. Mol Ecol 12:1113–1124.

Coburn RA, Griffin RH, Smith SD. 2015. Genetic basis for a rare floral mutant in an andean species of Solanaceae. Am J Bot 102:264–72.

Cooley AM, Modliszewski JL, Rommel ML, Willis JH. 2011. Gene duplication in mimulus underlies parallel floral evolution via independent trans-regulatory changes. Curr Biol 21:700–704.

Davies KM, Lewis DH, Winefield CS, Nielsen KM, Bradley JM, Schwinn KE, Deroles SC, Manson D, Jordan BR. 1997. Research into flower colour and flowering time in Eustoma grandiflorum (Lisianthus). Flower Newsl 23:24–32.

Dick CA, Buenrostro J, Butler T, Carlson ML, Kliebenstein DJ, Whittall JB. 2011. Arctic mustard flower color polymorphism controlled by petal-specific downregulation at the threshold of the anthocyanin biosynthetic pathway. PLoS One 6:.

Dunn CW, Luo X, Wu Z. 2013. Phylogenetic analysis of gene expression. Integr Comp Biol 53:847–856.

Gates DJ, Olson BJSC, Clemente TE, Smith SD. 2017. A novel R3 MYB transcriptional repressor associated with the loss of floral pigmentation in Iochroma. New Phytol 217:1346–1356.

Gerats AGM, Vlaming P de, Doodeman M, Al B, Schram AW. 1982. Genetic control of the conversion of dihydroflavonols into flavonols and anthocyanins in flowers of Petunia hybrida. Planta 155:364–368.

Gompel N, Prud'homme B. 2009. The causes of repeated genetic evolution. Dev Biol 332:36–47.

Grotewold E. 2006. The Science of Flavonoids. New York, NY: Springer Science & Business Media. 273 p.

Harborne JB. 1998. Phytochemical Methods: A Guide to Modern Techniques of Plant Analysis. London, UK: Chapman and Hall.

Hubbard JK, Uy JAC, Hauber ME, Hoekstra HE, Safran RJ. 2010. Vertebrate pigmentation: from underlying genes to adaptive function. Trends Genet 26:231–239.

Ives AR, Midford PE, Garland T. 2007. Within-species variation and measurement error in phylogenetic comparative methods. Syst Biol 56:252–70.

Kopp A. 2009. Metamodels and phylogenetic replication: A systematic approach to the evolution of developmental pathways. Evolution 63:2771–2789.

Larter M, Dunbar-Wallis A, Berardi AE, Smith SD. 2018. Convergent Evolution at the Pathway Level: Predictable Regulatory Changes during Flower Color Transitions. Mol Biol Evol 35:2159–2169.

Lavin SR, Karasov WH, Ives AR, Middleton KM, Garland Jr. T. 2008. Morphometrics of the Avian Small Intestine Compared with That of Nonflying Mammals: A Phylogenetic Approach. Physiol Biochem Zool 81:526–550.

Martin A, Orgogozo V. 2013. The loci of repeated evolution: A catalog of genetic hotspots of phenotypic variation. Evolution 67:1235–1250.

Massey JH, Wittkopp PJ. 2016. The Genetic Basis of Pigmentation Differences Within and Between Drosophila Species. Curr Top Dev Biol 119:27–61.

Nunes MDS, Arif S, Schlötterer C, McGregor AP. 2013. A perspective on micro-evo-devo: progress and potential. Genetics 195:625–34.

Peirson SN, Butler JN, Foster RG. 2003. Experimental validation of novel and conventional approaches to quantitative real-time PCR data analysis. Nucleic Acids Res 31:e73.

Pfaffl MW. 2001. A new mathematical model for relative quantification in real-time RT-PCR. Nucleic Acids Res 29:16–21.

Pollak PE, Vogt T, Mo Y, Taylor LP. 1993. Chalcone Synthase and Flavonol Accumulation in Stigmas and Anthers of Petunia hybrida. Plant Physiol 102:925–932.

R Core Team. 2019. R: A language and environment for statistical computing. R Foundation for Statistical Computing, Vienna, Austria. http://www.R-project.org/.'

Rausher, MD, Miller RE, Tiffin P. 1999. Patterns of evolutionary rate variation among genes of the anthocyanin biosynthetic pathway. Mol Biol Evol 16:266-274.

Rausher MD. 2006. The evolution of flavonoids and their genes. The Science of Flavonoids, p

175–211.

Rausher MD. 2013. The evolution of genes in branched metabolic pathways. Evolution 67:34–48.

Revell LJ. 2009. Size-correction and principal components for interspecific comparative studies. Evolution 63:3258–3268.

Revell LJ. 2012. phytools: An R package for phylogenetic comparative biology (and other things). Methods Ecol Evol 3:217–223.

Rogers WA, Williams TM, Salomone JR, Rebeiz M, Tacy DJ, Camino EM, Davis KA. 2013. recurrent modification of a conserved cis-regulatory element underlies fruit fly pigmentation diversity. PLoS Genet 9:e1003740.

Smith SD, Baum DA. 2006. Phylogenetics of the florally diverse Andean clade Iochrominae (Solanaceae). Am J Bot 93:1140–1153.

Smith SD, Goldberg EE. 2015. Tempo and mode of flower color evolution. Am J Bot 102:1014–1025.

Smith SD, Rausher MD. 2011. Gene loss and parallel evolution contribute to species difference in flower color. Mol Biol Evol 28:2799–2810.

Sobel JM, Streisfeld MA. 2013. Flower color as a model system for studies of plant evo-devo. Front Plant Sci 4:1–17.

Stern DL. 2000. Perspective: Evolutionary Developmental Biology and the Problem of Variation. Evolution 54:1079–1091.

Stern DL. 2011. Evolution, Development and the Predictable Genome. Greenwood Village: Roberts and Company Publishers.

Stern DL, Orgogozo V. 2009. Is genetic evolution predictable? Science 323:746–751.

Streisfeld MA, Rausher MD. 2011. Population genetics, pleiotropy, and the preferential fixation of mutations during adaptive evolution. Evolution 65:629–642.

Tanaka Y, Sasaki N, Ohmiya A. 2008. Biosynthesis of plant pigments: Anthocyanins, betalains and carotenoids. Plant J 54:733–749.

Whittall JB, Voelckel C, Kliebenstein DJ, Hodges SA. 2006. Convergence, constraint and the role of gene expression during adaptive radiation: Floral anthocyanins in Aquilegia. Mol Ecol 15:4645–57.

Winkel-Shirley B. 2001. Flavonoid biosynthesis. A colorful model for genetics, biochemistry, cell biology, and biotechnology. Plant Physiol 126:485–493.

Wittkopp PJ, Beldade P. 2009. Development and evolution of insect pigmentation: Genetic mechanisms and the potential consequences of pleiotropy. Semin Cell Dev Biol 20:65–71.

Wittkopp PJ, Stewart EE, Arnold LL, Neidert AH, Haerum BK, Thompson EM, Akhras S, Smith-Winberry G, Shefner L. 2009. Intraspecific polymorphism to interspecific divergence: genetics of pigmentation in Drosophila. Science 326:540–544.

Wray GA. 2007. The evolutionary significance of cis-regulatory mutations. Nat Rev Genet 8:206–216.

Wright KM, Rausher MD. 2010. The evolution of control and distribution of adaptive mutations in a metabolic pathway. Genetics 184:483–502.

Wu CA, Streisfeld MA, Nutter LI, Cross KA. 2013. The genetic basis of a rare flower color polymorphism in Mimulus lewisii provides insight into the repeatability of evolution. PLoS One 8.

Yuan Y-W, Rebocho AB, Sagawa JM, Stanley LE, Bradshaw HD. 2016. Competition between anthocyanin and flavonol biosynthesis produces spatial pattern variation of floral pigments between *Mimulus* species. Proc Natl Acad Sci 113:2448–2453.

**Figure legends**

**Figure 1. Simplified plant flavonoid biosynthesis pathway.** Diagram modified from Larter et al. (2018). Pathway enzymes are next to the arrows, and intermediate pathway products are in grey boxes. Abbreviations for enzymes are as follows: CHS (chalcone synthase), CHI (chalcone isomerase), F3H (flavanone-3-hydroxylase), FLS (flavonol synthase), FNS (flavone synthase), DFR (dihyroflavonol-4-reductase), ANS (anthocyanidin synthase). The three main classes of products are in the dashed boxes. The colored anthocyanidins are glycosylated to produce the final pigment products (anthocyanins). We found flavones in one only species in Iochrominae (*Dunalia solanacea*) and thus focus on the abundant flavonols and anthocyanins.

**Figure 2. Variation in floral flavonoids across Iochrominae.** Phylogeny from Smith and Goldberg (2015). Anthocyanins are shown with shaded bars and flavonols with white bars; error bars represent ± standard deviation. Polymorphic species (having pigmented and white morphs) are indicated with asterisks. Anthocyanin and flavonol content for the white morphs is displayed with bars outlined in gray as indicated in the legend. †*Vassobia breviflora* and *Iochroma confertiflorum* produce trace amounts of flavonols (Berardi et al. 2016; Larter et al. unpublished) although these were not detected in this HPLC analysis. *Dunalia solanacea* does not make flavonols or anthocyanidins but does make a moderate quantity of luteolin (a flavone); this data is included here descriptively but not in any subsequent analyses. Photos show representative pigmented and white individuals (from top to bottom): *Iochroma calycinum* (both morphs), *I. cyaneum* (pigmented species), *I. loxense* (white species), *I. parvifolium* (both morphs), and *Eriolarynx fasciculata* (both morphs).

**Figure 3. Relationship between floral anthocyanidin and flavonol concentration.** Each circle represents a species (closed for pigmented species, open for white species). Triangles represent data for the white morphs (averaged within each species); these were not included in the statistical analysis. The line and shaded area represent the best fit of a linear phylogenetic

regression and the 95% confidence interval obtained with parametric bootstrapping. This method takes phylogenetic non-independence into account, and incorporates within species variation (see Experimental Procedures). Data was log(x+1) transformed.

**Figure 4. Relationships between gene expression and flavonoid content.** Anthocyanin and flavonol concentrations were log(x+1) transformed. Expression values for two selected genes (the upstream *Chi* and the downstream *Ans*) are shown as log fold-change relative to a reference purple-flowered individual of *Iochroma cyaneum* (see Experimental Procedures). Symbols as in Fig. 3. Lines represent the best fit linear phylogenetic regressions and the shaded areas shows the 95% confidence intervals based on parametric bootstrapping. Analogous plots for other genes (*Chs*, *F3h*, and *Dfr*) can be generated through the scripts available in the associated Dryad Digital Repository: https://doi:10.5061/dryad.p5dq84v. Note that expression levels for *Dfr* and *Ans* are tightly correlated (Fig. 6B), and thus the graphs appear very similar.

**Figure 5. Gene expression profiles of white morphs and their pigmented conspecifics for the six polymorphic species.** Error bars show ± standard deviation across biological replicates (individuals) for each morph (pigmented and unpigmented) in each species. Note that only one white morph was found for *Iochroma calycinum* and for *I. parvifolium* (Table 1); thus, these columns have no error bars. Log fold-change gene expression was calculated relative to a reference purple-flowered individual of *I. cyaneum*.

**Figure 6. Phylogenetic PCA of gene expression for all individuals in this study (including white morphs). A**. Individual scores on the first two axes PC1 and PC2. **B**. Loadings of the gene expression variables on the same two axes. Symbols follow previous figures.

**Table 1. Sampling of species with morphs lacking floral anthocyanin pigments.** The number of individuals of each morph sampled in this study is given. The number of white morphs sampled depended on available flowering individuals, which are quite rare in some species. - Surveyed individuals (last column) include herbarium collections and natural populations.

| Polymorphic species | Phenotypes | # Sampled | Est. frequency of acyanic morph (# of individuals surveyed) |
|---|---|---|---|
| *Eriolarynx fasciculata* (Miers) Hunz. | purple/white | 3/3 | 1.8% (225) |
| *Iochroma calycinum* Benth. | purple/white | 3/1 | 0.9% (225) |
| *I. cyaneum* (Lindl.) M.L.Green | purple/white | 3/2 | 1.3% (150) |
| *I. parvifolium* (Roem. & Schult.) D'Arcy | purple/yellow | 3/1 | 1.3% (75) |
| *I. umbellatum* (Ruiz & Pav.) D'Arcy | purple/white | 3/3 | 57% (200) |
| *Saracha punctata* Ruiz & Pav. | purple/white | 3/2 | 33% (150) |

**Table 2. PGLS model selection and parameters for the five best models based on AIC scores.** Flavonoid type (anthocyanidins, top; flavonols, bottom) were modelled separately as functions of the gene expression of the pathway genes, alone or in multivariate models. Underlined and bold font indicates the best model for each pigment type. $\sigma^2$ and d are the variance and strength of selection parameters of the OU model of trait evolution (see Experimental Procedures for details).

| Anthocyanins (log-transformed) | Intercept | Slope *Chs* | Slope *Chi* | Slope *F3h* | Slope *Dfr* | Slope *Ans* | $\sigma^2$ | d | loglik | AIC | npar | ΔAIC |
|---|---|---|---|---|---|---|---|---|---|---|---|---|
| ***Chi*** | **0.31** | | **0.17** | | | | **0.12** | **0.75** | **-27.1** | **66.2** | **6** | **0.0** |
| *F3h* | 0.31 | | | 0.24 | | | 0.11 | 0.60 | -33.2 | 78.4 | 6 | 12.2 |
| [*Chi* + *F3h*] | 0.34 | | -1.59 | 1.69 | | | 0.08 | 0.43 | -36.0 | 92.0 | 10 | 25.8 |
| *Chs* | 0.31 | 0.08 | | | | | 0.12 | 0.71 | -41.2 | 94.4 | 6 | 28.2 |
| *Ans* | 0.34 | | | | | 0.20 | 0.09 | 0.30 | -53.6 | 119.3 | 6 | 53.1 |

| Flavonols (log-transformed) | Intercept | Slope *Chs* | Slope *Chi* | Slope *F3h* | Slope *Dfr* | Slope *Ans* | $\sigma^2$ | d | loglik | AIC | npar | ΔAIC |
|---|---|---|---|---|---|---|---|---|---|---|---|---|
| ***Chi*** | **0.45** | | **0.53** | | | | **0.08** | **0.97** | **-26.5** | **65.0** | **6** | **0.0** |
| *F3h* | 0.44 | | | 0.57 | | | 0.06 | 0.51 | -31.4 | 74.9 | 6 | 9.9 |
| [*Chi* + *F3h*] | 0.43 | | -0.49 | 0.98 | | | 0.07 | 0.50 | -35.3 | 90.6 | 10 | 25.6 |
| *Chs* | 0.44 | 0.29 | | | | | 0.09 | 0.84 | -41.3 | 94.7 | 6 | 29.7 |
| *Ans* | 0.43 | | | | | 0.08 | 0.10 | 0.88 | -58.0 | 128.0 | 6 | 63.0 |

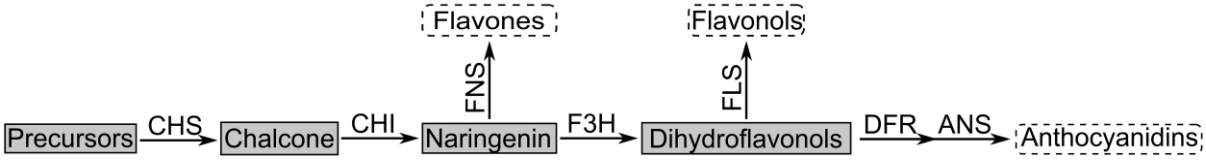




Developmental Dynamics

Developmental Dynamics

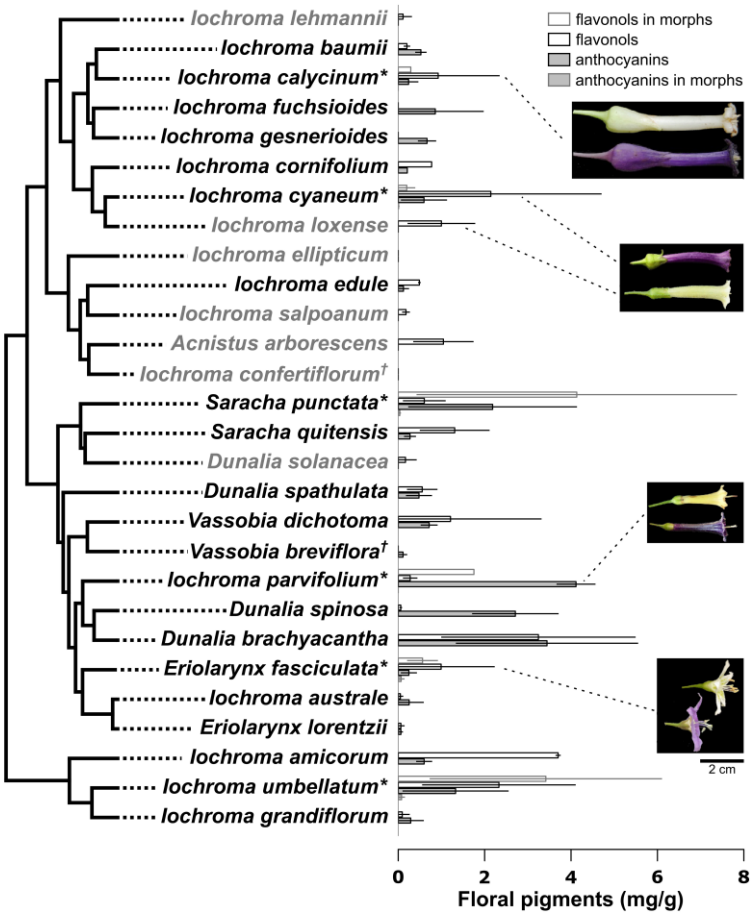

Developmental Dynamics

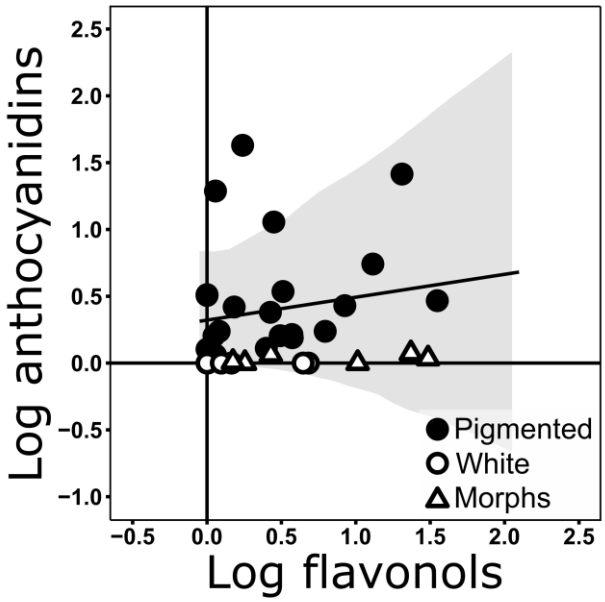

Developmental Dynamics

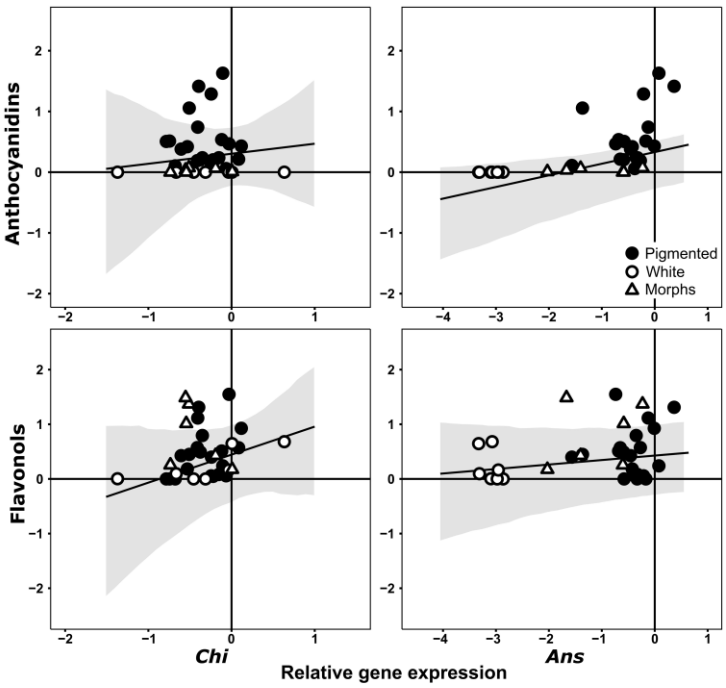

Developmental Dynamics

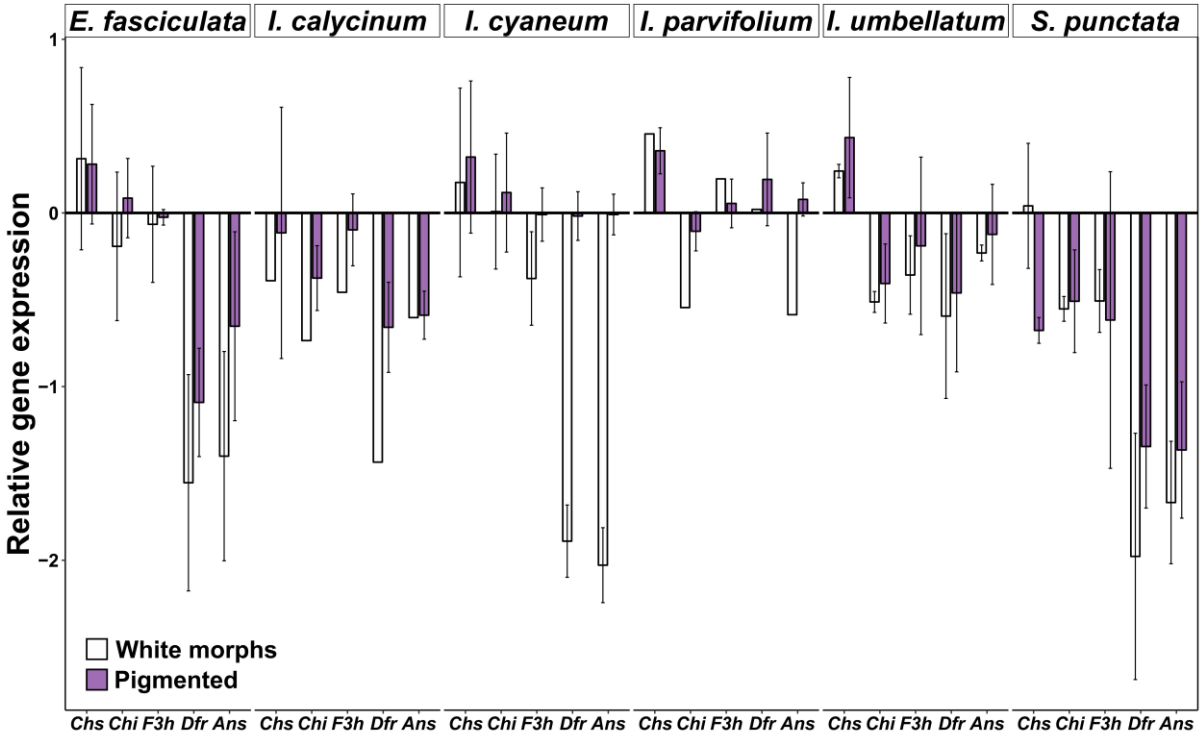

Developmental Dynamics